Journal of ELECTRONIC MATERIALS, Vol. 42, No. 4, 2013
DOI: 10.1007/s11664-012-2396-8

Transport Properties of Bulk Thermoelectrics—An International Round-Robin Study, Part I: Seebeck Coefficient and Electrical Resistivity

HSIN WANG,[1,11] WALLACE D. PORTER,[1] HARALD BÖTTNER,[2] JAN KÖNIG,[2] LIDONG CHEN,[3] SHENGQIANG BAI,[3] TERRY M. TRITT,[4] ALEX MAYOLET,[5] JAYANTHA SENAWIRATNE,[5] CHARLENE SMITH,[5] FRED HARRIS,[6] PATRICIA GILBERT,[7] JEFF W. SHARP,[7] JASON LO,[8] HOLGER KLEINKE,[9] and LASZLO KISS[10]

1.—Oak Ridge National Laboratory, Oak Ridge, TN, USA. 2.—Fraunhofer Institute for Physical Measurement Techniques, Freiburg, Germany. 3.—Shanghai Institute of Ceramics, Chinese Academy of Sciences, Shanghai, China. 4.—Clemson University, Clemson, SC, USA. 5.—Corning Inc., Corning, NY, USA. 6.—ZT-Plus Inc., Azusa, CA, USA. 7.—Marlow Industries, Dallas, TX, USA. 8.—CANMET, Hamilton, ON, Canada. 9.—University of Waterloo, Waterloo, ON, Canada. 10.—University of Quebec at Chicoutimi, Chicoutimi, QC, Canada. 11.—e-mail: wangh2@ornl.gov

Recent research and development of high-temperature thermoelectric materials has demonstrated great potential for converting automobile exhaust heat directly into electricity. Thermoelectrics based on classic bismuth telluride have also started to impact the automotive industry by enhancing air-conditioning efficiency and integrated cabin climate control. In addition to engineering challenges of making reliable and efficient devices to withstand thermal and mechanical cycling, the remaining issues in thermoelectric power generation and refrigeration are mostly materials related. The dimensionless figure of merit, *ZT*, still needs to be improved from the current value of 1.0 to 1.5 to above 2.0 to be competitive with other alternative technologies. In the meantime, the thermoelectric community could greatly benefit from the development of international test standards, improved test methods, and better characterization tools. Internationally, thermoelectrics have been recognized by many countries as a key component for improving energy efficiency. The International Energy Agency (IEA) group under the Implementing Agreement for Advanced Materials for Transportation (AMT) identified thermoelectric materials as an important area in 2009. This paper is part I of the international round-robin testing of transport properties of bulk thermoelectrics. The main foci in part I are the measurement of two electronic transport properties: Seebeck coefficient and electrical resistivity.

Key words: Thermoelectric, Seebeck coefficient, electrical resistivity, round-robin

INTRODUCTION

In the past decade, significant advances have been made to improve the interrelated transport properties of thermoelectrics.[1–3] In particular, materials with low thermal conductivity, high Seebeck coefficient, and low electrical resistivity have been developed to improve the figure of merit, *ZT*. While some research efforts have been focusing on low-dimensional materials, bulk thermoelectrics have shown the greatest potential in automotive applications. In bulk materials, the classic thermoelectric materials are bismuth telluride,[3] SiGe,[4] and

(Received August 31, 2012; accepted December 17, 2012; published online January 24, 2013)

lead telluride.[5] A new class of materials called skutterudites[6–12] emerged as one of the primary candidate materials for waste heat recovery after a 5-year study sponsored by the US Department of Energy.[13] Skutterudite is an example of Slack's[7] ideal thermoelectric material with the characteristics of phonon glass and electron crystal (PGEC). Other notable materials with high ZT values developed by various research groups are clathrates,[14–17] half-Heusler alloys,[18–28] $(GeTe)_{1-x}(AgSbTe_2)_x$ (TAGS),[5,29] lead-antimony-sliver-tellurium (LAST),[30–32] Zn_3Sb_4,[33–42] Mg and Mn silicides,[43–45] and oxides.[46–52] These materials have been among the top candidates for automotive applications since 2005.

The first round of selection to find the "best automotive-suited" material was based mainly on transport properties and ZT. During the selection process, some bulk materials were found to be unstable at high temperatures. The initial "good" properties could not be retained due to high-temperature exposure. Other materials were found "unfit" in the thermal and mechanical cycling environment. For example, PbTe is one of the materials used for radioisotope thermoelectric generators (RTGs) in space probes for the National Aeronautics and Space Administration (NASA).[6] It has been generating power successfully for tens of years under a constant temperature gradient. However, the same material was found to be damaged after several thermal cycles due to its weak mechanical strength and low resistance to thermal shock. Unless the mechanical strength of PbTe is improved, it might not be suitable for automotive applications in which thousands of thermal cycles are expected during service.

Another important selection issue recognized in the past 5 years to 6 years was the veracity of transport data. The successful design and development of thermoelectric modules and devices require accurate knowledge of transport properties, which is critical in the specifications and ultimate performance of the thermoelectric devices. However, some of the materials with good figure of merit reported in the literature could not be replicated or possessed much lower ZT than predicted. An early standardization effort was reported in the *Thermoelectric Handbook*.[53] Then, the material selected was skutterudite, and the two laboratories that participated in the efforts were University of Cardiff, UK and the German Aerospace Center (DLR), Germany. The Physical Properties Measurement System (PPMS by Quantum Design) at Aarhus University, Denmark was also used for low-temperature measurements. Although this study addressed the critical issues regarding transport property testing, the thermoelectric community did not take heed. This was likely because thermoelectrics were still in a research stage and the critical need for standardization becomes important during the transition stage from materials research to device manufacturing. Today, the same issues identified by the early study still exist and unreliable transport data continue to be reported in the literature. The reasons for unreliable transport properties may result from the following three issues:

1. Material nonuniformity: Thermal and electrical transport properties were not measured on a single sample in the same direction; the combination of the best properties tends to overestimate ZT.
2. Unrealistic extrapolation: Projections of low-temperature and room-temperature data to high temperatures were not valid.
3. Lack of standard test procedures and reference materials: Measurement errors and system mistakes were not recognized.

The participants in the International Energy Agency Advanced Materials for Transportation (IEA-AMT) annex VIII identified these issues in 2009 and started an international effort on transport property measurements through round-robin testing. The focus was on issue 3, i.e., the lack of test standards and test procedures. To address issues 1 and 2, homogeneous materials from a commercial source were used, and all the properties were measured in the same temperature range. To obtain the ZT value of a thermoelectric material over the application temperature range, five separate measurements might be conducted:

1. Thermal diffusivity (α in cm^2/s)
2. Specific heat (C_p in J/g·K)
3. Density (D in g/cm^3)
4. Seebeck coefficient (S in V/K)
5. Electrical resistivity (ρ in Ohm-m)

The product of items 1–3 gives the thermal conductivity,

$$k = 100 D \alpha C_p \quad (\text{in W m}^{-1}\,\text{K}^{-1}). \tag{1}$$

Since the density of the material is usually known or relatively easy to measure, only four potentially error-prone separate measurements are carried out to evaluate

$$ZT = S^2 T/\rho k \quad (\text{dimensionless}), \tag{2}$$

in which T is temperature in Kelvin. In the calculation of ZT, S^2/ρ is also known as the power factor. Alternatively, there are methods to measure k directly, especially below room temperature. These multiple transport measurements and the use of Eqs. 1 and 2 can significantly influence the accuracy of ZT.

The initial round-robin study on n-type and p-type bismuth telluride was completed in May 2010. It was clear that the timely effort by IEA-AMT addressed a very important issue to the international thermoelectric community. After analyzing the results and identifying measurement issues of

the first round-robin, a second round-robin study on *p*-type bismuth telluride was carried out and completed in August 2011. The low-temperature National Institute of Standards and Technology (NIST) standard reference material (SRM) for Seebeck coefficient from 10 K to 390 K became available in October 2011.[54,55] Although the cryogenic temperature range, sample geometry (8 mm tall), and the Seebeck-only nature of the NIST SRM prevented the IEA-AMT group from utilizing the same material, this IEA-AMT study used the same *n*-type Bi_2Te_3 composition provided by Marlow Industries, using a slightly different processing technique. The NIST SRM material values were compared with round-robin results in the overlapping temperature region. Part I of this study focuses on electrical properties: Seebeck coefficient and electrical resistivity.

SEEBECK COEFFICIENT

The Seebeck coefficient was introduced over 200 years ago by Thomas Seebeck.[56,57] The most recent reviews on Seebeck coefficient measurement are by Martin et al.,[58] and a California Institute of Technology group[59] recently developed a new apparatus for high-temperature Seebeck measurement. By definition, under a given temperature gradient and with no electrical current, the Seebeck coefficient is the ratio of the voltage drop ΔV along a temperature difference ΔT. Accurate measurements of the Seebeck coefficient require the temperature and voltage to be measured at the same location and the measured Seebeck value subtracted from the wires. Among the most common methods to measure the Seebeck coefficient, two methods are used.

Four-Point Method

In this method (Fig. 1a) no current is applied through the top and bottom electrodes, one of which is heated to generate a temperature gradient. Two thermocouples are usually used to measure temperatures by spring-loaded mechanical contact or direct bonding using conductive paste. Sometimes two small holes are drilled to embed the thermocouple leads. One wire of each thermocouple is also used as a voltage lead to obtain the voltage difference. This method can ensure that voltage and temperature can be measured at the same point. However, the contact wires can act as heat sinks causing measurement errors.

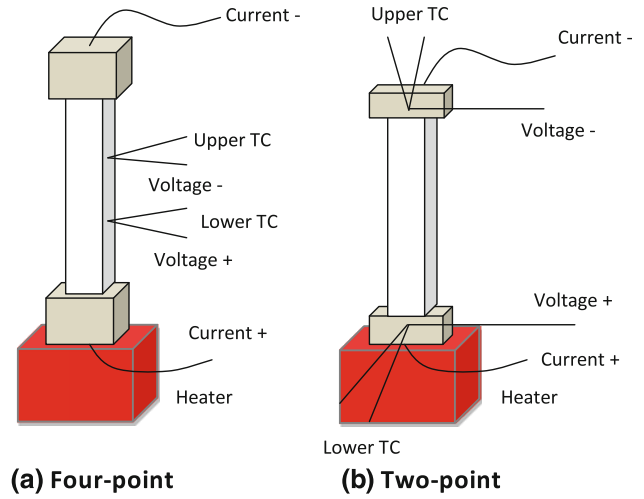

Fig. 1. (a) Four-point and (b) two-point measurement setups.

Two-Point Method

In this method (Fig. 1b) two electrodes are placed at the top and bottom of the specimen. The electrodes are often integrated as the hot- and cold-side heat sinks. Voltage leads and thermocouple wires need to be placed in the electrode. The measurements need to be as close to the contact surface as possible, and contacts must be of good quality, which is also the major source of measurement errors.

In thermoelectric research, both methods have been used and reported. The four-point method has been used more often, especially after the introduction of a commercial system by ULVAC-Riko. Since there were no standard Seebeck coefficient reference materials available until late 2011, calibrations of the Seebeck coefficient have relied on alloys such as constantan. The Seebeck values of constantan are 3 to 5 times lower than those of classic thermoelectrics such as bismuth telluride and lead telluride. A new SRM, especially in the higher temperature range (300 K to 800 K), will greatly benefit the thermoelectric community. Most participating laboratories are equipped with commercial instruments. There were not enough laboratories to use alternative techniques. Some techniques, such as the drilling and embedded contacts, were not practical for round-robin study. For the Seebeck calculations, most laboratories used the slope method instead of the ramping method. This is mainly due to the requirement to measure resistivity simultaneously. No temperature gradient should be present for resistivity measurements. The measurement atmosphere is usually helium or argon. The gas selection usually does not affect the results, but it is critical for the system to reach thermal equilibrium, especially near room temperature.

ELECTRICAL RESISTIVITY

Electrical resistivity (ρ in Ohm-m) is related to electrical conductivity (σ in Siemens/m) by a simple inverse relationship: $\sigma = 1/\rho$.

Electrical resistivity is a material property and for a rod- or rectangular-shaped sample is defined as $\rho = RA/l$, where A is the cross-sectional area and l is the length of the measured segment of material, and R is the measured resistance. For thermoelectric materials, electrical resistivity measurement is often coupled with Seebeck coefficient measurement. The same setups for Seebeck coefficient measurement in Fig. 1a, b are used.

The Peltier effect in thermoelectrics presents a special challenge to electrical resistivity measurement. The current passing through the specimen during resistivity measurement will induce an additional current, and the Joule heating effect will create measurement errors. The practical solution is to measure electrical resistivity before applying a temperature gradient to the specimen and to use fast switching of the polarity to cancel out the Peltier effect. It is believed that, due to the low thermal conductivity of most thermoelectric materials, the Peltier heating effect will take longer than typical measurement times, thus being only a minor source of error. The low-frequency AC technique[60,61] has been shown to be effective in canceling the unwanted Peltier contribution. Since the round-robin requires both Seebeck coefficient and resistivity measurements on the same samples and the known AC technique requires drilling holes for electrical contacts, no participating laboratory used the AC method.

Most electrical resistivity measurement errors come from the uncertainties of dimension measurements or contact resistance. In the two-point method, contact resistance could be a source of error for materials with high resistivity or metal–semiconductor nonohmic contact between the electrode and sample. In the four-point method, uncertainties of the locations of the center of the contact probe are a major source of error. The typical probe distance is from 4 mm to 8 mm. The dimensions of the contact tips, or conducting paste "dot," are on the order of 0.4 mm or larger. Taking the contact tips, for example, the true contact point could be at the edge if the tip is slightly bent. The uncertainty of the probe spacing alone could be 10% or higher.

MEASUREMENT SYSTEMS AND MATERIALS USED IN ROUND-ROBIN

In the round-robin tests, three measurement systems were used by participating laboratories:

- ULVAC ZEM-2 or ZEM-3 (four-point method)
- Laboratory system (two-point method)
- Modified Harman method

The basic round-robin rules were set as:

1. Each laboratory should use its normal practice to test the samples and report the results;
2. No laboratory will be identified in the reports;
3. The purpose of the round-robin is to identify testing issues, not to rank laboratory performance;
4. Round-robin data analysis may require system calibration data; failure to provide system calibration could result in the data not being included in the combined results.

n-Type and *p*-type nonproduction materials were made for round-robin testing by Marlow. The criteria for material selection were not the best *ZT*, but the best uniformity and consistency from sample to sample. The nominal composition of the *n*-type material is Bi_2Te_3 with slight excess Te, and the nominal composition of the *p*-type material is $Bi_{0.5}Sb_{1.5}Te_3$. The average grain size of the materials was about 20 μm.

To measure all the transport properties for *ZT* calculation, multiple sets of specimens (both *n*-type and *p*-type Bi_2Te_3) were prepared. Figure 2 shows one set of IEA-AMT specimens for measurement of electrical properties.

The specimens were prepared and machined to specifications by Marlow Industries:

1. *A subset of two n-type bismuth telluride specimens*

- A 2 mm × 2 mm × 15 mm bar for Seebeck coefficient and electrical resistivity tests
- A 3 mm × 3 mm × 12 mm bar for Seebeck coefficient and electrical resistivity tests

2. *A subset of two p-type bismuth telluride specimens*

- A 2 mm × 2 mm × 15 mm bar for Seebeck coefficient and electrical resistivity tests
- A 3 mm × 3 mm × 12 mm bar for Seebeck coefficient and electrical resistivity tests

FIRST INTERNATIONAL ROUND-ROBIN

One set of round-robin specimens were sent to each laboratory with instructions on temperature range. Each laboratory was asked to measure these samples to a maximum temperature of 498 K

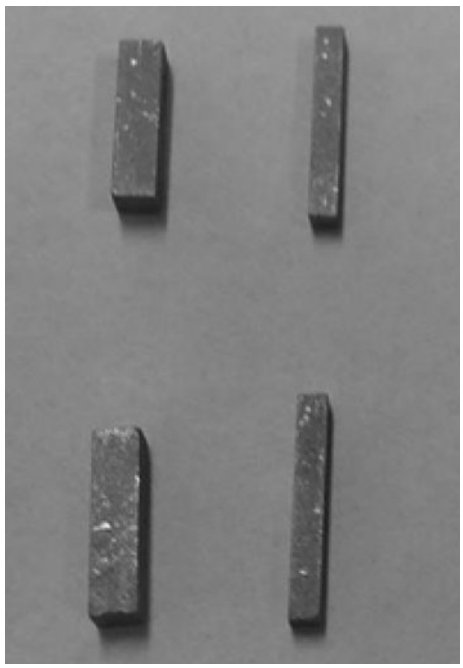

Fig. 2. Round-robin 1 samples sent to each laboratory: two *p*-type (top row) and two *n*-type (bottom row) samples.

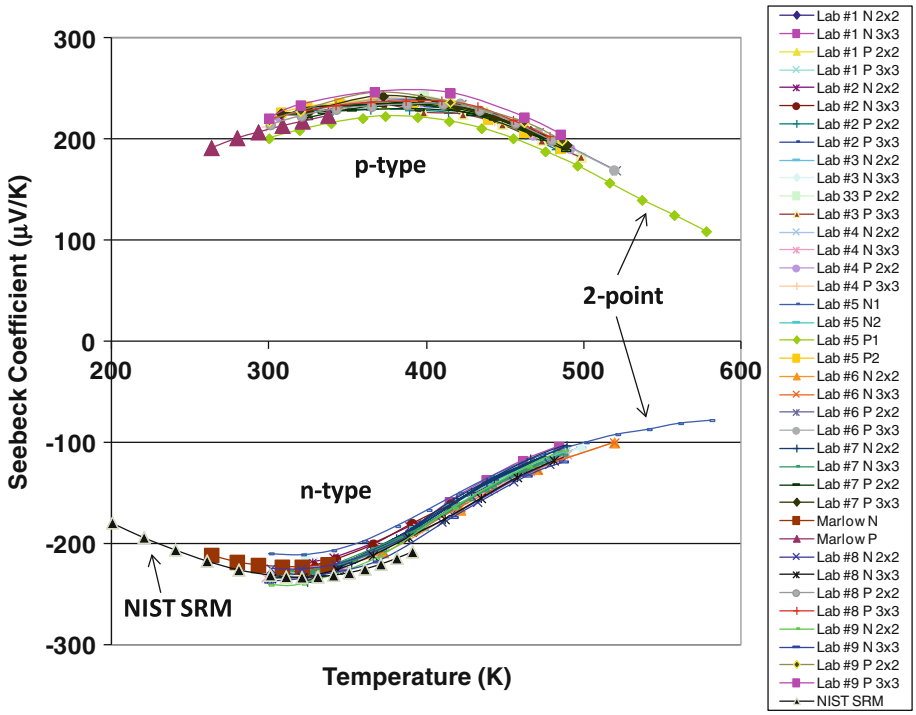

Fig. 3. Seebeck coefficient results of round-robin 1 from seven laboratories and Marlow.

starting from room temperature. No guidelines for testing procedures were given, and each laboratory was asked to perform the tests using their best practice. Specifically, the following instructions were sent to each laboratory for testing:

1. *Seebeck coefficient from 323 K to 498 K*: Each laboratory needs to describe the equipment used (in-house or commercial system). Parameters to report: current electrode material, voltage/thermocouple type, and test atmosphere. Measurement mode: set point with multiple ΔT or temperature ramping. Analysis: raw data and detailed analysis steps, corrections for probe Seebeck values.
2. *Electrical resistivity from 323 K to 498 K*: Use the same specimen as in test 1. Parameters to report: current electrode material, voltage/thermocouple type, specimen dimensions, voltage probe distance, and test atmosphere. Measurement mode: *I–V* test to confirm contact, ramping or set-point mode, current reversal, if ΔT exists during resistivity measurement. Analysis: how resistivity is determined at each temperature.

All participating laboratories performed Seebeck coefficient and electrical resistivity measurements. In the following discussion the laboratory identification numbers are not the same in each section. The laboratory identities were intentionally mixed because the main purpose of the round-robin was not to rank the performance of each laboratory but rather to identify all the issues related to measurements of transport properties of bulk thermoelectrics.

Seebeck Coefficient

Seebeck coefficient results from seven laboratories and Marlow are shown in Fig. 3. Three different types of instruments were used: ULVAC ZEM systems, modified Harman method, and a laboratory-made two-point system. The values for both *n*-type and *p*-type materials indicated that the Seebeck measurements produced consistent results among the participating laboratories. Data from NIST SRM 3451 are also plotted. It has the same true composition of *n*-type bismuth telluride as the samples from Marlow. The agreement with IEA-AMT materials is very good given that the materials were from a different batch with slight processing parameter variations. Among laboratories using the ULVAC ZEM system, the scatter was about ±4% for the short and long specimens. When the other two techniques are included, the scatter becomes about ±5.5%. The major difference comes from contact location and where temperature and voltage are measured. The ULVAC ZEM systems (four-probe method) seem to give a slightly higher absolute Seebeck value. The system using end contacts gave a slightly lower Seebeck value. The Marlow data obtained by modified Harman method (a Z-point setup) seem to be a good compromise, although it only measured data up to 343 K. The other source of error in Seebeck measurements may come from probe calibration. A correction value is needed to calculate the Seebeck coefficient as the probes are part of the measurement loop. Knowing the correct calibration value determines the measurement accuracy. However, the probe Seebeck values could

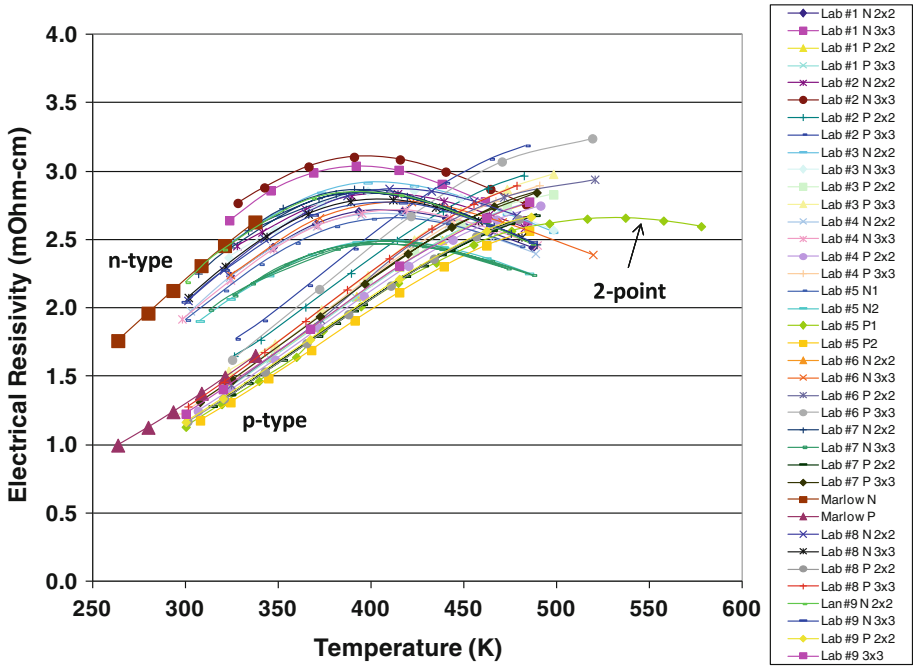

Fig. 4. Electrical resistivity results of round-robin 1 from seven laboratories and Marlow.

change after high-temperature exposures, especially when interdiffusion between the probe tips and thermoelectrics occur. The standard materials (constantan for ULVAC ZEM system) need to be periodically examined to monitor probe calibration drift.

Electrical Resistivity

Electrical resistivity results from seven laboratories and Marlow are shown in Fig. 4. Similar to Seebeck coefficient measurements, three different types of instruments were used, as these two properties are normally measured on the same specimen using the same probes. The resistivity results showed much larger scatter for both *p*-type and *n*-type specimens. The largest scatter for *n*-type material near 373 K was about ±12.5%. The scatter for the *p*-type material was smaller, although it seemed to show greater scatter at high temperatures. There was no clear difference between the short (3 mm × 3 mm × 12 mm) and long (2 mm × 2 mm × 15 mm) samples. However, the most significant errors were identified to come from the measurement and determination of probe distance. In some early ZEM systems the probe distance was not measured every time. Since the probe size is about 0.5 mm, this could easily introduce a 10% error in a measurement when the probe spacing is 5 mm. In the current model of ULVAC ZEM-3, a digital microscope is used to accurately measure the probe distance. Using the sample dimension measured by a micrometer as calibration in the captured image, the estimated accuracy of the digital microscope method is ±0.01 mm. The main source of error for electrical resistivity is the uncertainty of geometry measurements.

The first round-robin among seven laboratories using the Marlow Bi_2Te_3 was completed within 4 months. The study achieved its original goal, i.e., to identify problems in measurements of bulk transport properties. Using the commercially available materials and moderate temperature range, the IEA-AMT annex study observed the following:

1. Seebeck coefficient measurements showed very good agreement among the laboratories. The measurement errors were about ±5.5% for both types of materials and two sample geometries.
2. Electrical resistivity measurements of both *p*-type and *n*-type materials showed large errors. The largest error of ±12.5% occurred for the *n*-type material near 100°C. The uncertainty for dimension measurements was identified as the main source of error.

The round-robin 1 tests used Marlow hot-pressed materials. Although it is known to have consistent properties, it is still possible to have scatter due to localized material nonuniformity. Since each laboratory received a separate set of specimens, the possibility that errors were caused by the materials did exist. In order to understand the material uniformity, groups of 12 *n*-type and *p*-type Marlow materials were selected and tested at room temperature at Oak Ridge National Laboratory.

Figure 5 shows room-temperature electrical resistivity results of 12 *n*-type and 12 *p*-type samples. A four-point inline probe station by Signatone

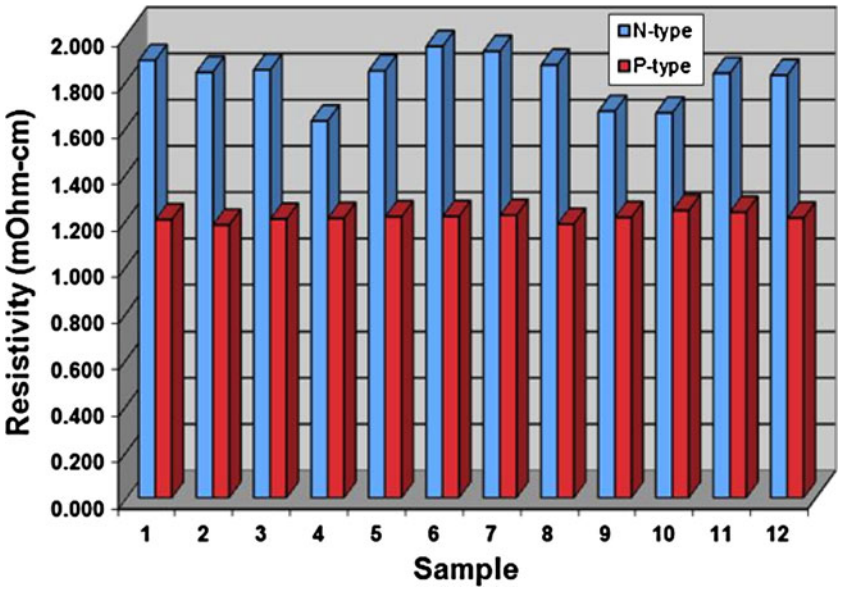

Fig. 5. Electrical resistivity of 12 *n*-type and 12 *p*-type samples at room temperature.

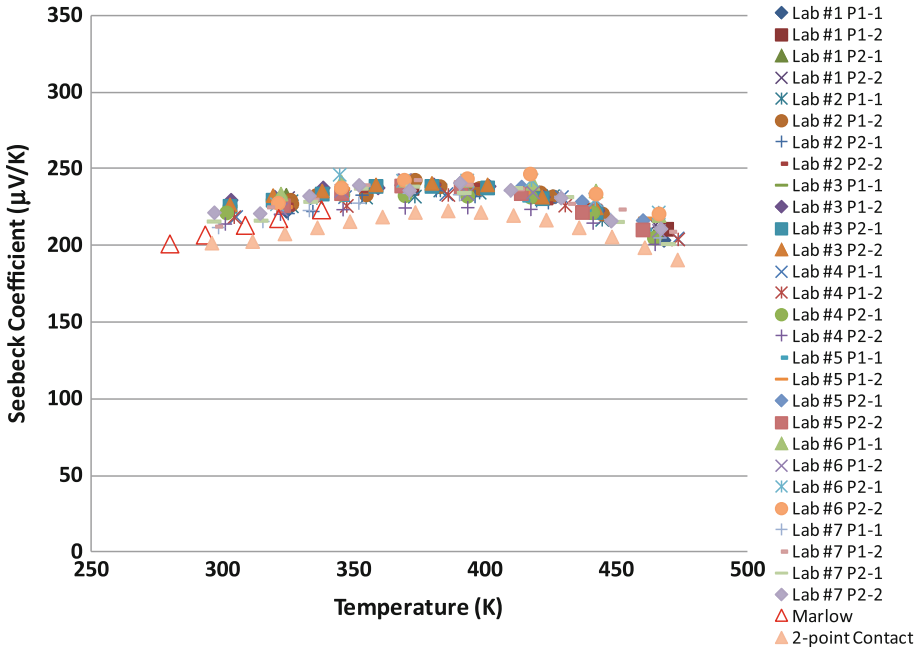

Fig. 6. Seebeck coefficient results of round-robin 2 for *p*-type bismuth telluride among seven laboratories.

was used. As shown in Fig. 5, the standard deviations were ±1.50% for *p*-type materials and ±5.81% for the *n*-type materials. Based on the above results, the *n*-type material showed larger sample-to-sample variations in electrical resistivity. This could have contributed to the measurement errors in round-robin 1, especially in the electrical resistivity results. It was determined by the annex participants to conduct a second round-robin using the *p*-type materials only.

SECOND INTERNATIONAL ROUND-ROBIN

Seebeck Coefficient

Seebeck coefficient results from seven laboratories and Marlow are shown in Fig. 6. Similar to round-robin 1, the agreement in Seebeck measurements was much better than other properties. All seven laboratories used ULVAC ZEM systems. One laboratory also ran the test using a laboratory-made system which used a different contact mechanism.

The Marlow data were obtained using modified Harman method on a 4 mm × 4 mm × 5 mm specimen. For all the ULVAC ZEM results, the scatter was about ±4% in the entire temperature range. The end-contact method gave lower Seebeck values. The Marlow Seebeck values lay in between the ULVAC values and end-contact values. Because of the size of the probes in the ULVAC system, it is possible to overestimate the Seebeck values. On the other hand, the end-contact method could be underestimating the Seebeck values. No large variations were observed in the Seebeck coefficient results.

Electrical Resistivity

Electrical resistivity results from seven laboratories and Marlow are shown in Fig. 7. All the data were obtained from simultaneous measurements with Seebeck coefficient. Each laboratory measured a long (2 mm × 2 mm × 15 mm) sample and a short sample (3 mm × 3 mm × 12 mm) for each set. The scatter was about ±5% near room temperature and increased to about ±9% at 473 K. A total of four specimens were measured by each laboratory. Not all the ZEM systems were equipped with the digital probe spacing measurement feature. Errors introduced by geometry measurements still exist. However, the increasing scatter at higher temperatures indicated that the measurements and data analysis have not been optimized. The Marlow data showed very good agreement with the round-robin results up to 343 K.

DATA SUMMARY AND TEST PROCEDURE

The results of the second international round-robin were analyzed to produce summarized results on Seebeck coefficient and electrical resistivity. Since the actual temperatures of each set of result are scattered, all the data points for Seebeck coefficient and electrical resistivity were plotted as a pool as shown in Figs. 8 and 9. The data scatter is the maximum spread of the data and is not the standard deviation. Since all the measurements were conducted at slightly different temperatures, it is not possible to apply standard statistical analysis. Better defined measurement temperature steps will be implemented in future round-robins to allow for better analysis. For the Seebeck coefficient of *p*-type bismuth telluride, a third-power polynomial curve fit was used to represent the temperature range from 293 K to 473 K:

$$S = -7E - 6T^3 - 0.0042T^2 + 0.0.2862T + 106.8 \ (\mu\text{V/K}), \quad (3)$$

in which S is the Seebeck coefficient and T is temperature in Kelvin. The data scatter over Eq. 3 is ±4.3%.

For electrical resistivity a linear curve fit was used:

$$\rho = 0.0094T - 1.587 \quad (\text{mOhm-cm}), \quad (4)$$

in which ρ is electrical resistivity and T is temperature in Kelvin.

The main purpose of this IEA-AMT study is to identify transport measurement issues and develop standard test procedures. A recommended test procedure for Seebeck coefficient and electrical resistivity has been completed and is shown below. This procedure will be updated as the high-temperature (300 K to 800 K) round-robin is completed in 2012.

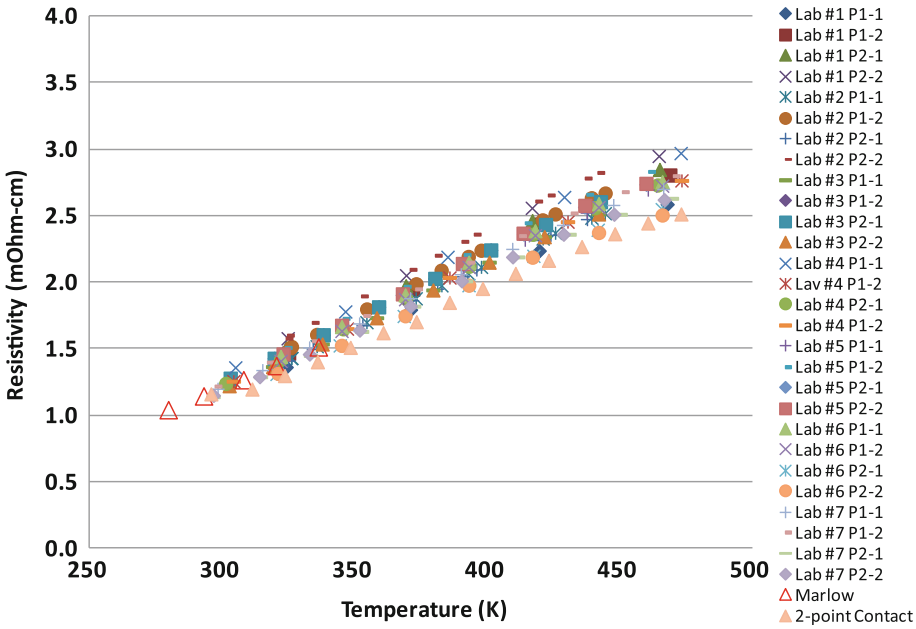

Fig. 7. Electrical resistivity results of round-robin 2 for *p*-type bismuth telluride among seven laboratories.

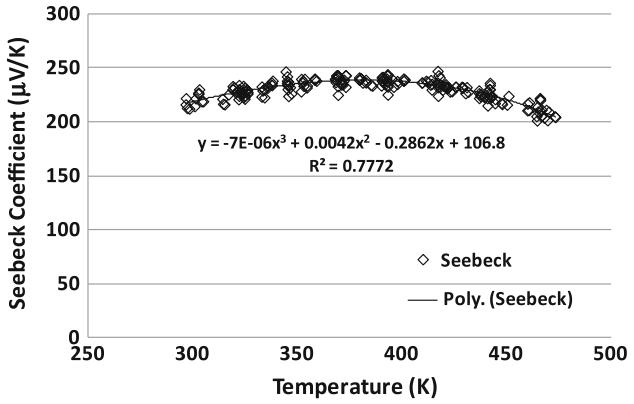

Fig. 8. Scattered data plot and curve fitting of Seebeck coefficient.

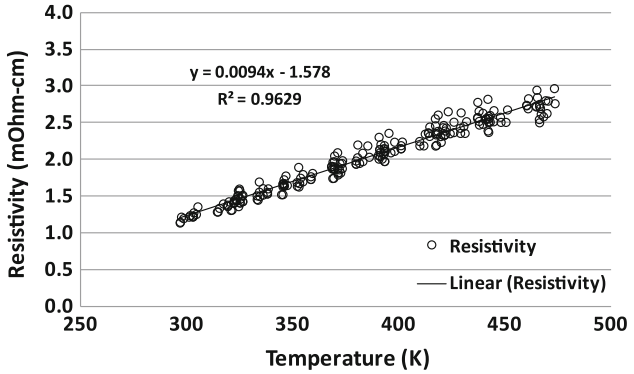

Fig. 9. Scattered data plot and curve fitting of electrical resistivity.

TEST PROCEDURE FOR SEEBECK COEFFICIENT AND ELECTRICAL RESISTIVITY

The standard Seebeck coefficient and electrical resistivity tests are performed on a single specimen. The test procedures for simultaneous measurements are described below:

Specimen

The standard Seebeck coefficient and electrical resistivity tests are performed on a single specimen. The ideal specimen is a long cylinder or bar. For typical thermoelectrics, geometries such as a 2 mm × 2 mm × 15 mm bar or a 3 mm × 3 mm × 12 mm bar are sufficient. Due to the large percentage probe distance error in resistivity measurements on shorter samples, it is recommended that the sample length be larger than 10 mm. The specimens need to be machined with parallel surfaces. The top and bottom surfaces need to be flat and parallel to ensure good contacts. Specimen dimensions need to be determined using a calibrated micrometer. The voltage probe spacing needs to be determined for each measurement. A better solution is to use a digital microscope, with the measured sample width used as calibration from the same image. The center-to-center distance of the voltage probes is used in the calculation.

Seebeck Coefficient and Resistivity Tests

The Seebeck coefficient and resistivity measurements are usually performed using the potentiometric (four-probe) or the axial flow (two-probe) method. For high-temperature measurements, the test environment is usually vacuum, very low-pressure static helium or flowing argon. Seebeck coefficient can be measured by slowly ramping the furnace or using the differential method in which the sample is stabilized at a set point and a small ΔT is applied across the specimen. To determine Seebeck coefficient several ΔT settings are used and the slope of the ΔV versus ΔT curve gives the total Seebeck coefficient of the circuit. To obtain the true Seebeck value of the specimen, the Seebeck value of the probe material needs to be subtracted. The values for the probe are available for the thermocouple used (K or R type) and provided as a lookup table.

In the differential method, it is preferred to measure electrical resistivity before the ΔT is established at each set point for Seebeck measurements. Due to the Joule heating and Peltier effect of thermoelectrics, a temperature gradient may be generated and cause measurement error. In order to eliminate this effect, the current is usually reversed quickly without altering the voltage measurement polarity. However, in order to minimize the Peltier effect, the measurements must be completed within 1 s or even faster.

There are other techniques to measure electrical resistivity such as the four-point probe (inline probes) or the van der Pauw technique.[62] For the inline probe method, it is important to recognize that the measurement is more accurate for isotropic thin specimens. Measurements on materials with layered structures, such as Bi_2Te_3, must be analyzed carefully since resistivity depends on orientation and how the specimen is cut. The van der Pauw technique is suitable for very thin specimens (<0.5 mm), and it is also a surface resistivity measurement.

Calibration

The Seebeck values are less dependent on sample geometry. However, it is common practice to place the probes away from the current contact to avoid nonuniform heat areas. The system should be calibrated using a reference material with known Seebeck values (such as constantan for certain commercial systems). The Seebeck values of the measured references need to be within the specified accuracy limits. If there is drift outside the acceptable range, a new probe is needed.

CONCLUSIONS

The international round-robin study by IEA-AMT is a timely effort to enable the commercialization of thermoelectric devices, especially for automotive

applications. Using hot-pressed *n*-type and *p*-type bismuth telluride materials from Marlow Industries, measurement issues for Seebeck coefficient and electrical resistivity have been identified. The two round-robin studies among four countries and eight laboratories showed very good agreement in Seebeck coefficient measurements but much larger uncertainty in electrical resistivity data. It was identified that probe distance determination is the main source of error. A standard test procedure for Seebeck coefficient and electrical resistivity has been developed. In part II of this paper, thermal conductivity measurements will be discussed and the final evaluation of *ZT* will be presented.

ACKNOWLEDGEMENTS

The authors would like to thank the International Energy Agency under the Implementing Agreement for Advanced Materials for Transportation for supporting this work, the assistant secretary for Energy Efficiency and Renewable Energy of the Department of Energy and the Propulsion Materials Program under the Vehicle Technologies Program. We would like to thank all participating institutions and Oak Ridge National Laboratory managed by UT-Battelle LLC under contract DE-AC05000OR22725 for support.

REFERENCES

1. A.F. Ioffe, *Semiconductor Thermoelements and Thermoelectric Cooling* (London: Infosearch, 1957).
2. J.C. Peltier, *Ann. Chem.* LVI, 371 (1834).
3. H.J. Goldsmid, *Electronic Refrigeration* (London: Pion Limited, 1986).
4. D.M. Rowe, eds., *CRC Handbook of Thermoelectrics* (Boca Raton, FL: CRC, 1995).
5. G.S. Nolas, J. Sharp, and H.J. Goldsmid, *Thermoelectrics: Basic Principles and New Materials Developments* (New York: Springer, 2001).
6. Jet Propulsion Laboratory Thermoelectric Science and Engineering Web Site, http://www.its.caltech.edu/~jsnyder/thermoelectrics/. Accessed August 20, 2012.
7. G.A. Slack, *CRC Handbook of Thermoelectrics*, ed. D.M. Rowe (Boca Raton, FL: CRC, 1995), p. 407.
8. G.S. Nolas, G.A. Slack, and S.B. Schujman, *Semicond. Semimet.* 69, 255 (2000).
9. B.C. Sales, D. Mandrus, and R.K. Williams, *Science* 272, 1325 (1996).
10. B.C. Sales, D.G. Mandrus, and B.C. Chakoumakos, *Semicond. Semimet.* 70, 1 (2001).
11. D.T. Morelli and G.P. Meisner, *J. Appl. Phys.* 77, 3777 (1995).
12. C. Uher, *Semicond. Semimet.* 69, 139 (2000).
13. C. Keppens, D. Mandrus, B.C. Sales, B.C. Chakoumakos, P. Dai, R. Coldea, M.B. Maple, D.A. Gajewski, E.J. Freeman, and S. Bennington, *Nature* 395, 876 (1998).
14. V.L. Kuznetsov, L.A. Kuznetsova, A.E. Kaliazin, and D.M. Rowe, *J. Appl. Phys.* 87, 7871 (2000).
15. G.S. Nolas, *Thermoelectrics Handbook: Macro- to Nano-Structured Materials*, edited by D.M. Rowe (Boca Raton, FL: CRC Press, 2005), pp. 33-1.
16. W. Jeischko, *Metall. Trans. A* 1, 3159 (1970).
17. S.J. Poon, *Recent Trends in Thermoelectric Materials Research II*, ed. T.M. Tritt, *Semiconductors and Semimetals*, vol. 70, chap. 2, Treatise Editors, R.K. Willardson and E.R. Weber (New York: Academic Press, 2001), p. 37.
18. J. Tobola, J. Pierre, S. Kaprzyk, R.V. Skolozdra, and M.A. Kouacou, *J. Phys. Condens. Matter* 10, 1013 (1998).
19. F.G. Aliev, N.B. Brandt, V.V. Moschalkov, V.V. Kozyrkov, R.V. Scolozdra, and A.I. Belogorokhov, *Phys. B Condens. Matter* 75, 167 (1989).
20. S. Ogut and K.M. Rabe, *Phys. Rev. B* 51, 10443 (1995).
21. W.E. Pickett and J.S. Moodera, *Phys. Today* 54, 39 (2001).
22. C. Uher, J. Yang, S. Hu, D.T. Morelli, and G.P. Meisner, *Phys. Rev. B* 59, 8615 (1999).
23. H. Hohl, A.P. Ramirez, C. Goldmann, G. Ernst, B. Wolfing, and E. Bucher, *J. Phys. Condens. Matter* 11, 1697 (1999).
24. S. Sportouch, P. Larson, M. Bastea, P. Brazis, J. Ireland, C.R. Kannenwurf, S.D. Mahanti, C. Uher, and M.G. Kanatzidis, *Thermoelectric Materials 1998—The Next Generation Materials for Small-Scale Refrigeration and Power Generation Applications*, ed. T.M. Tritt, M.G. Kanatzidis, G.D. Mahan, and H.B. Lyon, Jr. (Warrendale, PA: Mater. Res. Soc. Symp. Proc. 545, 1999), p. 421.
25. S. Bhattacharya, A.L. Pope, R.T. Littleton IV, T.M. Tritt, V. Ponnambalam, Y. Xia, and S.J. Poon, *Appl. Phys. Lett.* 77, 2476 (2000).
26. Y. Xia, S. Bhattacharya, V. Ponnambalam, A.L. Pope, S.J. Poon, and T.M. Tritt, *J. Appl. Phys.* 88, 1952 (2000).
27. Q. Shen, L. Chen, T. Goto, T. Hirai, J. Yang, G.P. Meisner, and C. Uher, *Appl. Phys. Lett.* 79, 4165 (2001).
28. S. Sakurada and N. Shutoh, *Appl. Phys. Lett.* 86, 2105 (2005).
29. E. Skrabeck and D.S. Trimmer, *CRC Handbook of Thermoelectrics*, ed. D.M. Rowe (Boca Raton, FL: CRC, 1995), p. 267.
30. K.F. Hsu, S. Loo, F. Guo, W. Chen, J.S. Dyck, C. Uher, T. Hogan, E.K. Polychroniadis, and M.G. Kanatzidis, *Science* 303, 818 (2004).
31. S. Sportouch, M. Bastea, P. Brazis, J. Ireland, C.R. Kannewurf, C. Uher, and M.G. Kanatzidis, *Thermoelectric Materials 1998—The Next Generation Materials for Small-Scale Refrigeration and Power Generation Applications*, ed. T.M. Tritt, M.G. Kanatzidis, G.D. Mahan, and H.B. Lyon, Jr. (Warrendale, PA: Mater. Res. Soc. Symp. Proc. 545, 1999), p. 123.
32. E. Quarez, K.F. Hsu, R. Pcionek, N. Frangis, E.K. Polychroniadis, and M.G. Kanatzidis, *J. Am. Chem. Soc.* 127, 9177 (2005).
33. H.W. Mayer, I. Mikhail, and K. Schubert, *J. Less-Common Met.* 59, 43 (1978).
34. T. Caillat, J.-P. Fleurial, and A. Borshchevsky, *J. Phys. Chem. Solids* 58, 1119 (1997).
35. V.L. Kuznetsov and D.M. Rowe, *J. Alloys Compd.* 372, 103 (2004).
36. S.C. Ur, I.H. Kim, and P. Nash, *Mater. Lett.* 58, 2132 (2004).
37. K. Ueno, A. Yamamoto, T. Noguchi, T. Inoue, S. Sodeoka, H. Takazawa, C.H. Lee, and H. Obara, *J. Alloys Compd.* 385, 254 (2004).
38. G.J. Snyder, M. Christensen, E. Nishibori, T. Caillat, and B.B. Iversen, *Nat. Mater.* 3, 458 (2004).
39. M. Tsutsui, L.T. Zhang, K. Ito, and M. Yamaguchi, *Intermetallics* 12, 809 (2004).
40. F. Cargnoni, E. Nishibori, P. Rabiller, L. Bertini, G.J. Snyder, M. Christensen, and B.B. Inversen, *Chem. Eur. J.* 20, 3861 (2004).
41. S.G. Kim, I.I. Mazin, and D.J. Singh, *Phys. Rev. B* 57, 6199 (1998).
42. J. Nylen, M. Andersson, S. Lidin, and U. Haeussermann, *J. Am. Chem. Soc.* 126, 16306 (2004).
43. V.K. Zaitsev, M.I. Fedorov, E.A. Gurieva, I.S. Eremin, P.P. Konstantinov, A.Y. Samunin, and M.V. Vedernikov, *Phys. Rev. B* 74, 045207 (2006).
44. M. Fukano, T. Iida, K. Makino, M. Akasaka, Y. Oguni, and Y. Takanashi, *Thermoelectric Power Generation*, ed. T. P. Hogan, J. Yang, R. Funahashi and T. Tritt (MRS Proceedings Vol. 1044, 2007), U06-13.
45. N.L. Okamoto, T. Koyama, K. Kishida, K. Tanaka, and H. Inui, *Acta Mater.* 57, 5036 (2009).

46. I. Terasaki, Y. Sasago, and K. Uchinokura, *Phys. Rev. B* 56, R12685 (1997).
47. R. Funahashi, I. Matsubara, H. Ikuta, T. Takeuchi, U. Mizutani, and S. Sodeoka, *Jpn. J. Appl. Phys. Pt.* 2, L1127 (2000).
48. A.C. Masset, C. Michel, A. Maignan, M. Hervieu, O. Toulemonde, F. Studer, B. Raveau, and J. Hejtmanek, *Phys. Rev. B* 62, 166 (2000).
49. Y. Miyazaki, K. Kudo, M. Akoshima, Y. Ono, Y. Koike, and T. Kajitani, *Jpn. J. Appl. Phys. Pt.* 2, L531 (2000).
50. A. Satake, H. Tanaka, T. Ohkawa, T. Fujii, and I. Terasaki, *J. Appl. Phys.* 96, 931 (2004).
51. M. Shikano and R. Funahashi, *Appl. Phys. Lett.* 82, 1851 (2003).
52. I. Matsubara, R. Funahashi, T. Takeuchi, S. Sodeoka, T. Shimizu, and K. Ueno, *Appl. Phys. Lett.* 78, 362 (2001).
53. E. Muller, C. Stiewe, D.M. Rowe, and S.G.K. Williams, *CRC Thermoelectric Handbook*, 2nd ed., Chapter 26 (Boca Raton: CRC, 2006), pp. 1–3.
54. NIST SRM 3451, Low Temperature Seebeck Coefficient Standard (10 K to 390 K) (2011).
55. N.D. Lowhorn, W. Wong-Ng, Z.Q. Lu, J. Martin, M.L. Green, E.L. Thomas, J.E. Bonevich, N.R. Dilley, and J. Sharp, *J. Mater. Res.* 26, 1983–1992 (2011).
56. E. Velmre, *Proc. Estonian Acad. Sci. Eng.* 13, 276 (2007).
57. T.J. Seebeck, Aus den Jahren 1822 und 1823, pp. 265–373 (1825). Extracts from four lectures delivered at the Academy of Sciences in Berlin on August 16 (1821), October 18 and 25 (1821), and February 11 (1822).
58. J. Martin, T. Tritt, and C. Uher, *J. Appl. Phys.* 108, 121101 (2010).
59. S. Iwanaga, E.S. Toberer, A. LaLonde, and G.J. Synder, *Rev. Sci. Instrum.* 82, 1–6 (2011).
60. M.A. Logan, *Bell Syst. Tech. J.* 40, 885 (1960).
61. Z. Zhou and C. Uher, *Rev. Sci. Instrum.* 76, 023901 (2005).
62. L.J. van der Pauw, *Philips Res. Rep.* 13, 1–9 (1958).